

Effect of Chloride Ion Concentration on the Corrosion Behavior of 304 Stainless Steel Used in the Electric Water Heater

Zhong Yin

Guangdong Midea Group Kitchen & Bathroom Appliance Manufacturing Co., Ltd., Foshan 528311, Guangdong Province, China

E-mail: ZYin_Media@163.com

Received: 19 December 2021 / Accepted: 8 February 2022 / Published: 4 March 2022

In this paper, the effect of chloride ion concentration on the corrosion behavior of 304 stainless steel used in the electric water heater at 25 °C and 80 °C is investigated, by using open circuit potential tests, electrochemical impedance spectroscopy (EIS), polarization curves tests. It is found that the passive film can be spontaneously formed at the corrosion potential. The E_{ocp} values of 304 stainless steel progressively stabilize at 25 °C, while the E_{ocp} values are unstable at 80 °C. The chloride ion in the solution is detrimental for forming protective oxides passive film both at 25 °C and 80 °C, due to the increase of Q_1 -Y values and the decrease of R_1 values with the increase of chloride ion concentration. However, the impedances increase with the immersion time at 25 °C, while the impedances increase at the beginning of the immersion (1 hour→1 day), and then gradually decrease with the increase of immersion time at 80 °C. In addition, the E_{corr} and E_{pit} tend to noble with the decrease of the concentration of chloride ion at the same temperature. The E_{pit} at 25 °C is much nobler than that at 80 °C in the same solution. The radius and depths of the pits formed on the surface after polarization curve tests increase with the increase of concentration of chloride ions.

Keywords: Electric water heater, Stainless steel, Corrosion resistance, Chloride ion

1. INTRODUCTION

Water heater is an essential home appliances for modern families. Recently, the storage type electric water heater has attracted increasing attention when compared to gas water, due to the requirements of low carbon emission which was put forward in the Paris Climate Agreement [1]. As a core component of electric water heater, the inner tank is generally fabricated by economical corrosion-resistant enamel-coated carbon steel or stainless steel [2, 3]. In this industry, the stainless steel inner tanks seem owning a better development potential, because of their more reliably corrosion performance and lightweight [4-6]. However, the corrosion perforation is still have to be guarded treated.

Stainless steel is a typical iron based alloy with outstanding corrosion resistance, which contains at least 10.5 wt. % chromium and several other alloyed elements such as Ni, Mn, et al [7, 8]. Generally, the high corrosion resistance of stainless steels is attributed to the nature barrier properties of easily formed passive film on the surface [9-12]. However, the stainless steels are susceptible to localized attack in acids and chlorides-containing solution [13-17]. Generally, the research of stainless steels are mainly focus on the seawater which contains high content of chloride ion at room temperature. However, it is still lack of study on electrochemical corrosion behavior of stainless steels in the domestic water with low content of chloride ion at high temperature.

Nowadays, our company's products (Midea) has been all over the world, there exists different chloride ion concentration in the tap water of different area. Even in the domestic water with low concentration chlorides, it is possible that the stability of the passive film of the stainless steels would be influenced. To improve the stability of the products, the effect of chloride ion concentration on the corrosion behavior of 304 stainless steel used in the electric water heater has been investigated in this study by various electrochemical techniques [18]. In addition, considering that the temperature of the water in the inner tank would reach to 80 °C or higher when the electric water heater is operating, and the temperature is close to room temperature when the power goes out, two solution temperature (25°C and 80 °C) have been studied in this paper.

2. EXPERIMENTAL

The 304 stainless steel samples (11 mm × 11 mm × 1 mm) used in this study were drawn from the electric water heater (Media, China). Then, the obtained quadrature samples were polished with 400 to 2000 grit SiC waterproof abrasive papers and then ultrasonic cleaned in the acetone and deionized water, respectively. Thereafter, the samples were dried by cold air. The chemical composition examined by inductively coupled plasma atomic emission spectrometer (ICP-AES, Optima-7000DV, Thermofisher) is showed in Table 1.

Table 1. Chemical composition of 304 stainless steel used in this study (wt.%).

| Ni | Cr | Mo | Cu | Mn | Si | C | P | S | Fe |
|------|-------|------|------|------|------|-------|-------|-------|------|
| 8.09 | 18.07 | 0.15 | 0.36 | 1.06 | 0.34 | 0.057 | 0.032 | 0.002 | Bal. |

The 304 stainless steel samples were encapsulated by epoxy resin to confirm that the test area exposed to the solution is 1 cm². All electrochemical tests were conducted on a workstation (PARSTAT VersaSTAT 3F) with three-electrode system. The counter electrode is Pt sheet (20 mm×20 mm), the reference electrode is saturated-calomel electrode (SCE) and the working electrode is the encapsulated 304 stainless steel samples. The test solution was the synthetic tap water with different concentration of chloride ion (200 ppm, 500 ppm, 1000 ppm). In this paper, the 3.5 wt.% NaCl solution which is close to the seawater was also used as the test solution for a more critical assessment. The chemical composition

of tested solutions is listed in Table 2. The pH value was adjusted to about 7.2 by using 0.5 M H₂SO₄ solution, and tests were conducted at 25 ± 1 °C (room temperature) and 80 ± 1 °C (i.e., the maximum water temperature inner the electric water heater).

Table 2 The chemical composition of the test solution (ppm)

| <i>Solution</i> | Cl ⁻ | SO ₄ ²⁻ | HCO ₃ ⁻ | Ca ²⁺ | Mg ²⁺ |
|-----------------|-----------------|-------------------------------|-------------------------------|------------------|------------------|
| <i>A</i> | 200 | 0.74 | 1.21 | 0.003 | 0.023 |
| <i>B</i> | 500 | 0.74 | 1.21 | 0.003 | 0.023 |
| <i>C</i> | 1000 | 0.74 | 1.21 | 0.003 | 0.023 |
| <i>D</i> | 3.5 wt.% NaCl | | | | |

Prior to each electrochemical testing process, the 304 stainless steel samples should be immersed in the solution for 60 min to attain a relatively steady surface state. The electrochemical impedance spectroscopy (EIS) measurement was conducted at the corrosion potential with an AC disturbance signal of 10 mV (rms) in the frequency region of 99 kHz-10 mHz and the impedance data were analyzed using the ZsimpWin software. The anode polarization curves were performed from -0.05 V vs. OCP to the potentials when current density reached to 10⁻³ A cm⁻², with a scan rate of 10 mV min⁻¹. All electrochemical tests were repeated at least three times with different specimens.

3. RESULTS AND DISCUSSION

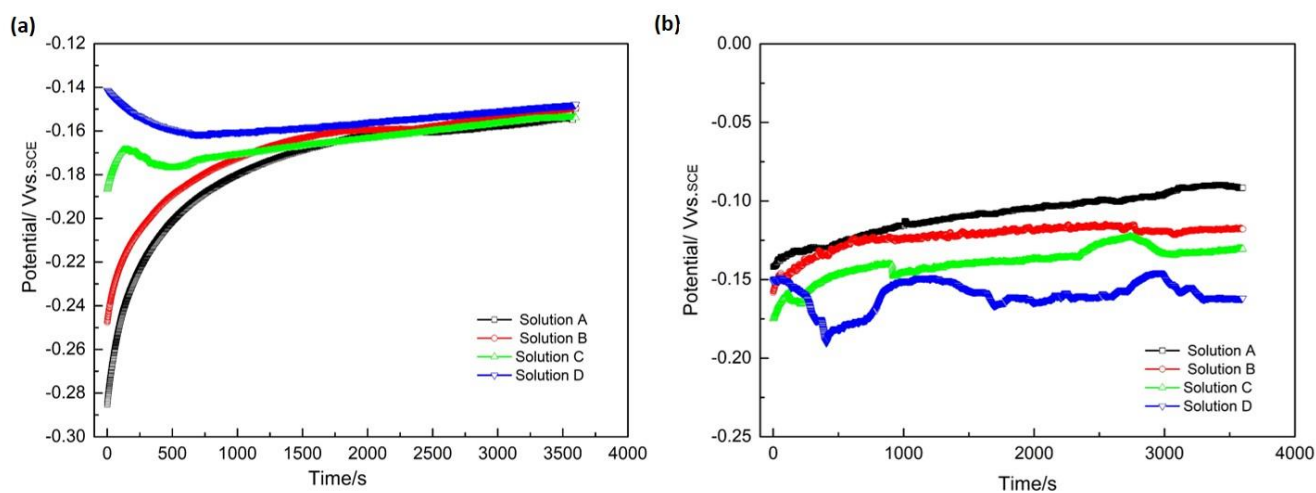


Figure 1. Open circuit potential of 304 stainless steel as a function of time in different solutions at (a) 25 °C and (b) 80 °C

Fig. 1 presents the variation of the open circuit potential, E_{ocp} , of 304 stainless steel immersed into the synthetic tap water with different chloride ion concentration and the 3.5 wt.% NaCl solution. When the solution temperature is 25 °C, it is clearly that the E_{ocp} significantly increases with time in the early stage, and then progressively stabilizes when the 304 stainless steel specimen immersed into the synthetic tap water (Fig. 1a). However, the E_{ocp} decreases with time at the beginning of the immersion and then tends to be stable in the 3.5 wt.% NaCl solution (Fig. 1a). The decrease of the E_{ocp} could be attributed to a destruction of the native oxide film on 304 stainless steel in the solution with high concentration of chloride ion (3.5 wt.% NaCl) [19].

The E_{ocp} values are nobler than the initial values and could be stable after immersed into the solution 1500s at 25 °C, suggesting that the protective passive films can be formed on the surface of 304 stainless steel [20]. However, the E_{ocp} values are unstable at 80 °C, especially in the 3.5 wt.% NaCl solution. It means the formed passive film are metastable and causes breakdown in local areas [21, 22]. To obtain more reliable information about the long-term environmental stability of protective films, EIS measurements and anode polarization curves are performed.

Fig. 2 shows the Nyquist plots for the specimens with different immersion time and in different solutions at 25 °C. Clearly, the values of impedance ($|Z|$) increase with the immersion time in all of the solutions. Besides, the increase of the impedances are mainly contributed by the increase of the imaginary part of the impedance ($-Z$), which is related to the constantly forming of passive film [23, 24]. In addition, the impedance increase with the decrease of the concentration of chloride ion, indicating that the chloride ion in the solution is adverse for forming protective passive film.

In order to calculate the electrochemical parameters, an electrical equivalent circuit (EEC) displayed in Fig. 3 was used to fit the experimental data. In this EEC, R_s is the solution resistance; Q_1 and Q_2 are the constant phase element (CPE) for analyzing the frequency dispersion behavior of different corrosion phenomena caused by surface heterogeneity, R_1 represents charge-transfer of the oxides formed on the surface, R_{ct} represents the faradic resistance [25]. The fitted results are listed in Table 2, the chi-square values (Σc^2 , $10^{-4} \sim 10^{-3}$, order of magnitudes) are very small, confirming the good fitting quality. It should be mentioned that the R_s values are not listed in Table 2, because all the obtained R_s values are less than 100 Ω , which are much smaller than the R_1 and R_{ct} values and could be neglected. It can be found that the values of Q_1-Y_0 , which is the proportionality factor for CPE impedance, are gradually decreasing with the increase of immersion time, indicating that the thickness of oxides film increased with immersion time [26]. Meanwhile, and the R_1 values also increase with immersion time. It means that the protective films can formed and the film would become thicker with immersion time when the solution temperature is 25 °C. In addition, with the increase of chloride ion concentration in the solution, the Q_1-Y values increase and the R_1 values also decrease, demonstrating the chloride ion is adverse for the formation of protective oxides film (passive films).

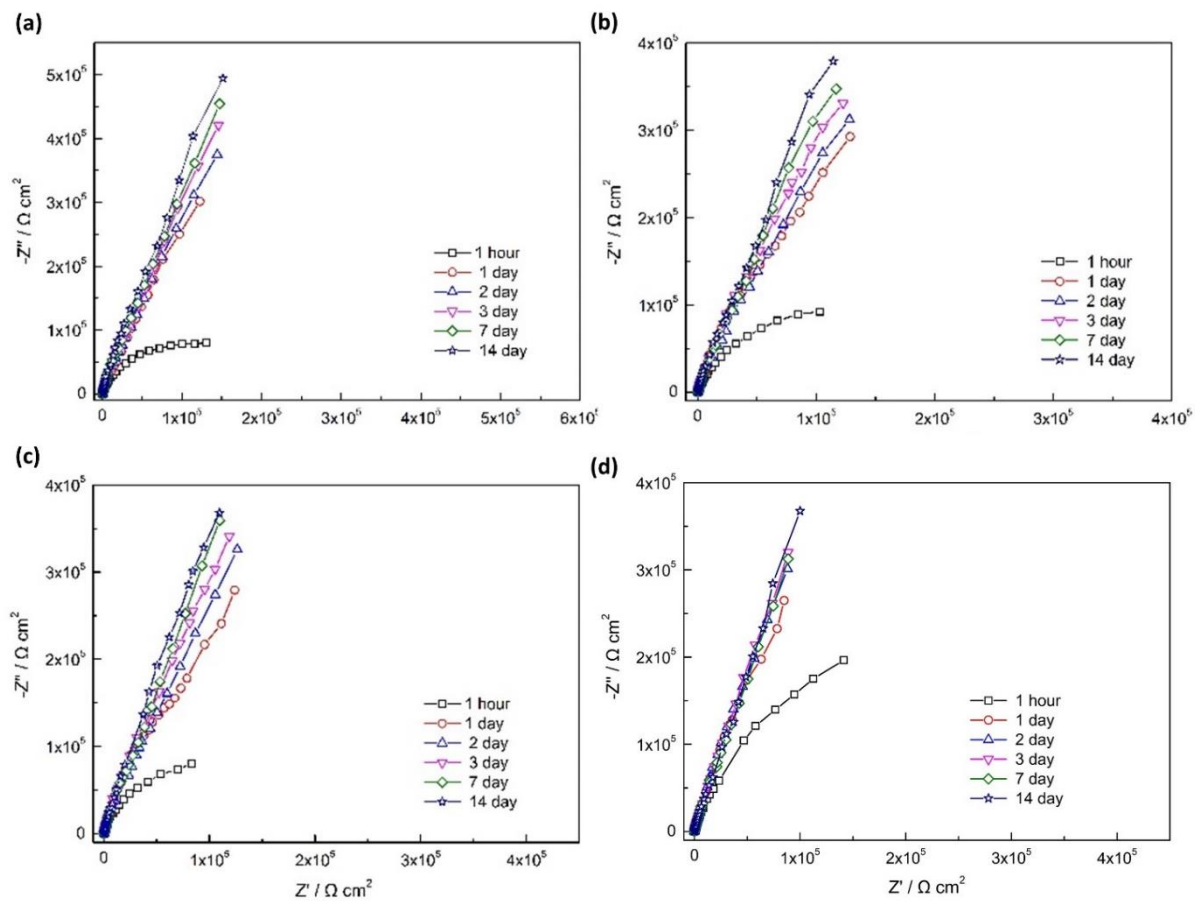


Figure 2. Nyquist plots for the specimens at 25 °C with different immersion time and in different solutions: (a) Solutions-A, (b) Solutions-B, (c) Solutions-C (d) Solutions-D.

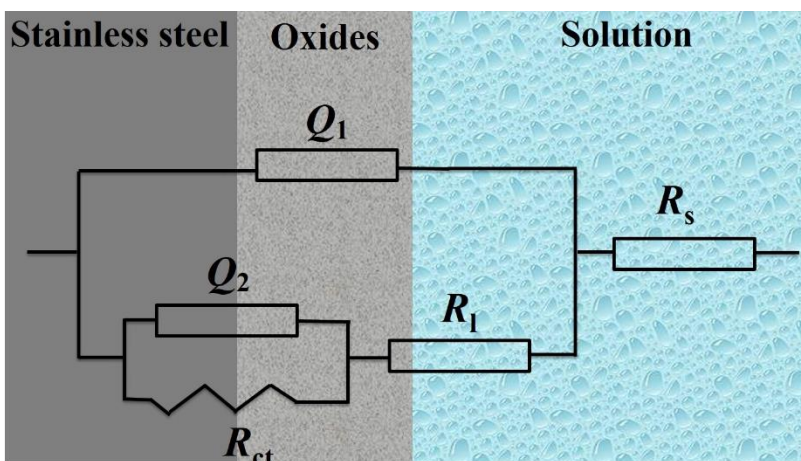


Figure 3. The electrical equivalent circuit (EEC) for fitting the EIS experimental data.

Table 3. The equivalent circuit parameters for impedance spectra in Fig. 2

| Solution | Time | Q_1-Y_0 ($10^{-5} \Omega^{-1} \text{cm}^{-2} \text{s}^n$) | n_1 | R_1 ($\text{k}\Omega \text{cm}^2$) | Q_2-Y_0 ($10^{-5} \Omega^{-1} \text{cm}^{-2} \text{s}^n$) | n_1 | R_{ct} ($\text{k}\Omega \text{cm}^2$) | Σc^2 ($\times 10^{-4}$) |
|----------|--------|--|-------|---|--|-------|--|--------------------------------------|
| A | 1 hour | 2.95 | 0.85 | 49 | 1.61 | 0.82 | 190 | 7.5 |
| | 1 day | 2.12 | 0.88 | 403 | 1.57 | 0.93 | 243 | 1.6 |
| | 2 day | 1.81 | 0.90 | 471 | 1.17 | 0.93 | 250 | 2.1 |
| | 3 day | 1.74 | 0.92 | 559 | 1.10 | 0.94 | 380 | 4.3 |
| | 7 day | 1.62 | 0.91 | 664 | 0.91 | 0.95 | 382 | 1.5 |
| | 14 day | 1.51 | 0.92 | 816 | 0.78 | 0.95 | 426 | 3.0 |
| B | 1 hour | 5.34 | 0.86 | 58 | 4.54 | 0.86 | 218 | 4.5 |
| | 1 day | 4.95 | 0.88 | 250 | 3.99 | 0.87 | 253 | 8.8 |
| | 2 day | 3.65 | 0.89 | 405 | 3.58 | 0.90 | 282 | 1.7 |
| | 3 day | 2.96 | 0.92 | 570 | 2.74 | 0.91 | 369 | 1.1 |
| | 7 day | 2.30 | 0.94 | 535 | 2.11 | 0.93 | 395 | 1.8 |
| | 14 day | 1.93 | 0.93 | 602 | 1.74 | 0.93 | 463 | 2.9 |
| C | 1 hour | 8.48 | 0.92 | 57 | 8.09 | 0.89 | 125 | 1.3 |
| | 1 day | 7.94 | 0.03 | 230 | 6.32 | 0.91 | 143 | 9.8 |
| | 2 day | 6.81 | 0.91 | 447 | 4.77 | 0.92 | 361 | 6.4 |
| | 3 day | 5.56 | 0.94 | 518 | 3.70 | 0.92 | 386 | 1.0 |
| | 7 day | 5.34 | 0.93 | 556 | 3.42 | 0.95 | 394 | 4.9 |
| | 14 day | 4.65 | 0.94 | 638 | 2.16 | 0.94 | 1.17 | 7.5 |
| D | 1 hour | 8.39 | 0.92 | 46 | 10.52 | 0.88 | 159 | 3.5 |
| | 1 day | 7.16 | 0.92 | 190 | 9.58 | 0.88 | 173 | 1.3 |
| | 2 day | 6.97 | 0.93 | 326 | 8.10 | 0.87 | 266 | 11.0 |
| | 3 day | 6.71 | 0.95 | 386 | 8.05 | 0.91 | 340 | 1.2 |
| | 7 day | 6.07 | 0.93 | 418 | 7.52 | 0.92 | 378 | 9.0 |
| | 14 day | 5.68 | 0.95 | 471 | 6.93 | 0.91 | 415 | 1.5 |

Fig. 4 displays the Nyquist plots for the specimens with different immersion time and in different solutions at 80 °C. It can be found that the impedance decrease with the increase of the concentration of chloride ion, which is the same with that at 25 °C. However, the impedance ($|Z|$) increase at the beginning of the immersion (1 hour→1 day), and then gradually decrease with the increase of immersion time in all of the solutions at 80 °C (1 day→14 day). This means, the passive film are instability and would gradually dissolve and lose the protection. The EEC showed in Fig. 3 is employed to fit the experimental data and the results are listed in Table 4. It is clearly that the chi-square values are also small. The Q_1-Y_0 values increase and the R_1 values decrease with immersion time when the immersion time is more than 1 day, meaning that the oxides films would be dissolved and destroyed in the long time immersion process at high temperature (80°C). In addition, it can also be found that the chloride ion is detrimental for forming protective oxides passive film, due to the increase of Q_1-Y values incorporation with the decrease of R_1 values (shown in Table 4). However, the Q_1-Y values at 80°C are much bigger that at 25°C, and R_1

values at 80°C are much smaller than at 25°C, confirming the high temperature solution would result in dissolution of oxides films and accelerate corrosion.

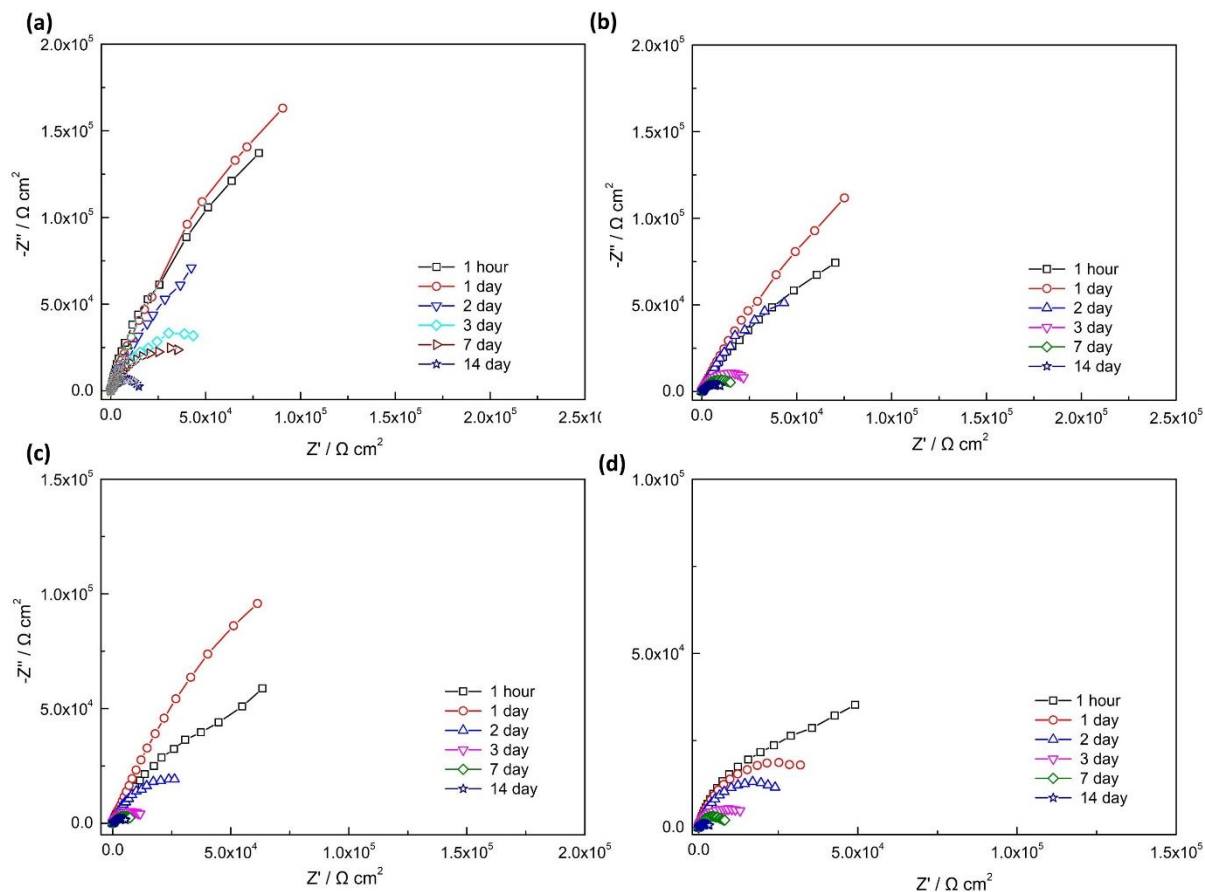


Figure 4. Nyquist plots for the specimens at 80 °C in different solutions: (a) Solutions-A, (b) Solutions-B, (c) Solutions-C, (d) Solutions-D.

Table 4. The equivalent circuit parameters for impedance spectra in Fig. 4

| Solution | Time | Q_1-Y_0 ($10^{-5} \Omega^{-1} \text{cm}^{-2} \text{s}^n$) | n_1 | R_1 ($\text{k}\Omega \text{cm}^2$) | Q_2-Y_0 ($10^{-5} \Omega^{-1} \text{cm}^{-2} \text{s}^n$) | n_1 | R_1 ($\text{k}\Omega \text{cm}^2$) | Σc^2 ($\times 10^{-4}$) |
|----------|--------|--|-------|---|--|-------|---|--------------------------------------|
| A | 1 hour | 8.78 | 0.87 | 68 | 7.43 | 0.79 | 155 | 1.3 |
| | 1 day | 8.69 | 0.89 | 88 | 7.38 | 0.81 | 196 | 5.3 |
| | 2 day | 10.84 | 0.85 | 56 | 8.09 | 0.85 | 129 | 4.4 |
| | 3 day | 12.24 | 0.82 | 42 | 8.68 | 0.84 | 97 | 3.7 |
| | 7 day | 15.06 | 0.82 | 35 | 9.23 | 0.82 | 83 | 2.3 |
| | 14 day | 16.55 | 0.81 | 31 | 10.07 | 0.85 | 32 | 1.3 |
| B | 1 hour | 9.02 | 0.91 | 58 | 8.03 | 0.91 | 146 | 3.9 |
| | 1 day | 8.16 | 0.90 | 78 | 7.32 | 0.90 | 199 | 6.0 |

| | | | | | | | | |
|---|--------|--------|------|----|--------|------|-----|------|
| | 2 day | 9.85 | 0.88 | 58 | 8.23 | 0.88 | 89 | 1.7 |
| | 3 day | 11.17 | 0.87 | 46 | 9.30 | 0.83 | 73 | 2.3 |
| | 7 day | 13.54 | 0.81 | 30 | 14.02 | 0.77 | 57 | 4.5 |
| | 14 day | 18.21 | 0.79 | 26 | 29.45 | 0.78 | 37 | 15.3 |
| C | 1 hour | 10.43 | 0.86 | 45 | 10.01 | 0.81 | 119 | 5.0 |
| | 1 day | 9.14 | 0.82 | 67 | 15.71 | 0.81 | 138 | 8.3 |
| | 2 day | 11.95 | 0.75 | 47 | 9.41 | 0.79 | 75 | 17.4 |
| | 3 day | 17.40 | 0.76 | 28 | 16.83 | 0.77 | 45 | 1.8 |
| | 7 day | 21.88 | 0.79 | 17 | 47.08 | 0.76 | 24 | 2.5 |
| | 14 day | 50.32 | 0.78 | 9 | 65.88 | 0.75 | 21 | 1.7 |
| D | 1 hour | 15.88 | 0.86 | 36 | 13.06 | 0.74 | 123 | 3.8 |
| | 1 day | 11.03 | 0.82 | 54 | 10.83 | 0.76 | 61 | 1.8 |
| | 2 day | 27.10 | 0.87 | 19 | 16.44 | 0.81 | 36 | 5.3 |
| | 3 day | 43.97 | 0.82 | 11 | 29.97 | 0.80 | 17 | 6.6 |
| | 7 day | 80.08 | 0.80 | 9 | 67.59 | 0.81 | 10 | 12.8 |
| | 14 day | 150.87 | 0.81 | 4 | 109.07 | 0.78 | 6 | 4.7 |

Fig. 5 presents the polarization curves for the specimens in different solutions at 25 °C and 80 °C. As shown, all the polarization curves change directly into passive region without the transition of active to passive, meaning that the passive films can be spontaneously formed at the corrosion potential. The corresponding corrosion electrochemical parameters extracted from the polarization curves are listed in Table 5. It shows that both the corrosion potentials (E_{corr}) and pit potentials (E_{pit}) tend to be nobler with the decrease of the concentration of chloride ion at the same solution temperature. In addition, in the same solution, the E_{pit} at 25 °C is much nobler than that at 80 °C, suggesting that the passive films formed at 80 °C would become less stable. These results are highly in correspondence with results which are extracted from E_{ocp} -t cures (Fig. 1) and EIS plots (Fig. 2, Fig. 4).

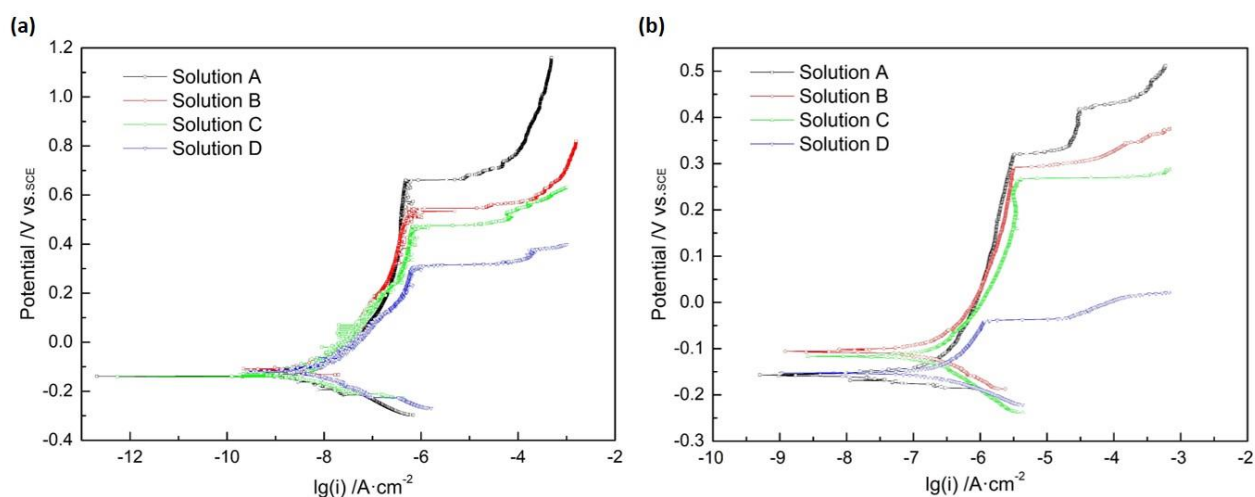


Figure 5. Polarization curves for the specimens in different solution at (a) 25 °C and (b) 80 °C

Table 5. The electrochemical parameters extracted from the polarization curves in Figs. 5.

| Temperature (°C) | Solutions | E_{corr} (mV) | i_{corr} ($\mu\text{A}\cdot\text{cm}^{-2}$) | E_{pit} (mV) | i_{pass} ($\mu\text{A}\cdot\text{cm}^{-2}$) |
|------------------|-----------|-----------------|---|----------------|---|
| 25 | A | -137 | 0.14 | 662 | 4.36 |
| | B | -114 | 0.18 | 543 | 5.50 |
| | C | -142 | 0.19 | 485 | 6.32 |
| | D | -125 | 0.87 | 304 | 7.20 |
| 80 | A | -158 | 0.74 | 319 | 26.91 |
| | B | -106 | 1.25 | 295 | 27.52 |
| | C | -112 | 1.82 | 267 | 31.66 |
| | D | -175 | 3.98 | 450 | 20.44 |

Fig. 6 shows the SEM morphologies of the specimen surface after polarization measurement at 25°C. It is seen that the pits formed on the surfaces of 304 stainless steel in synthetic tap water with different concentration of chloride ions at 25 °C (Fig. 6a-c). While the pits are quite evident in the 3.5 wt. % NaCl solution at this temperature (Fig. 6d). However, there exist particularly obvious pits on the surface of 304 stainless steel when the solution temperature is 80°C (shown in Fig. 7). In addition, it can be found that the radius and depths of the pits are increase with the increase of concentration of chloride ions [27]. Therefore, it can be concluded that the 304 stainless steel couldn't exhibit excellent pitting corrosion resistance at the working temperature for electric water heater (80 °C) in comparison with that at room temperature (25 °C), even in the tap water. In addition, the chloride ion in the tap water are is adverse for the corrosion resistance of 304 stainless steel used in electric water heater.

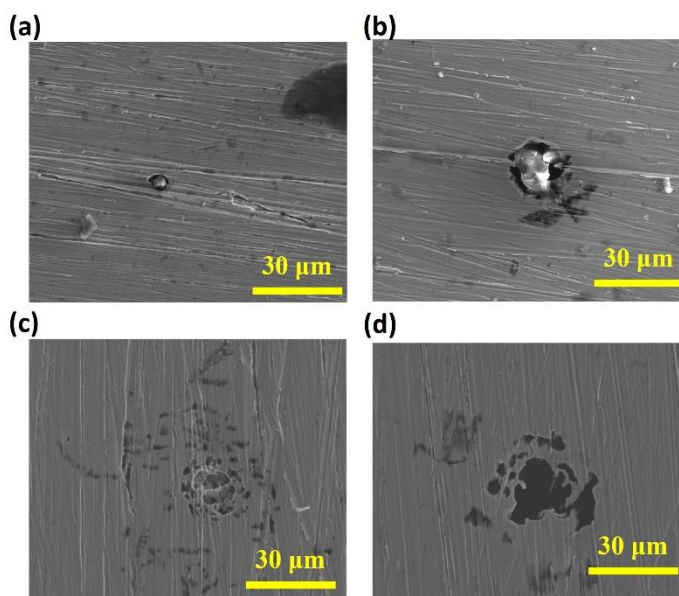


Figure 6. SEM morphologies of the specimen surfaces after the polarization measurement at 25 °C in different solutions: (a) Solutions-A, (b) Solutions-B, (c) Solutions-C (d) Solutions-D.

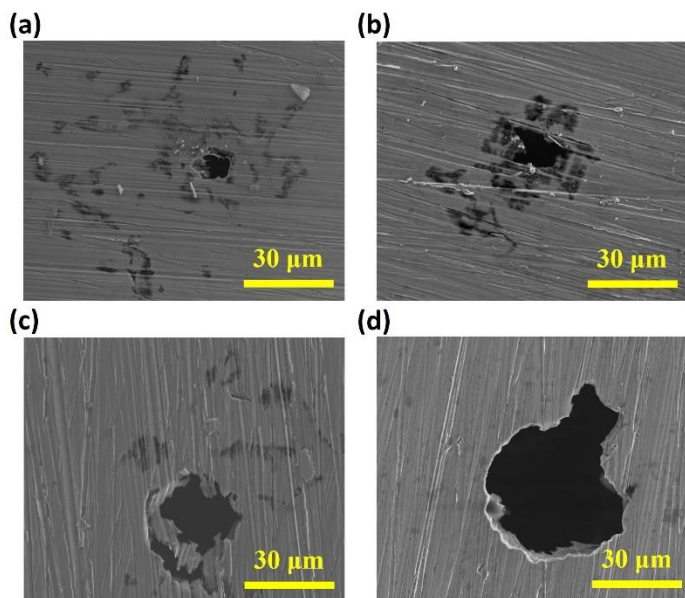


Figure 7. SEM morphologies of the specimen surfaces after the polarization measurement at 80 °C in different solutions: (a) Solutions-A, (b) Solutions-B, (c) Solutions-C (d) Solutions-D.

4. CONCLUSIONS

In this paper, the effect of chloride ion concentration on the corrosion behavior of 304 stainless steel used in the electric water heater at 25 °C and 80 °C is investigated. Conclusions can be drawn as follows:

- (1) The E_{ocp} values of 304 stainless steel specimen progressively stabilizes when the solution temperature is 25 °C, while the E_{ocp} values are unstable at 80 °C, especially in the 3.5 wt.% NaCl solution.
- (2) The chloride ion in the solution is detrimental for forming protective oxides passive film both at 25 °C and 80 °C, due to the increase of Q_1 -Y values and the decrease of R_1 values with the increase of chloride ion concentration.
- (3) The values of impedance increase with the immersion time in all of the solutions at 25 °C. The impedance increase at the beginning of the immersion (1 hour→1 day), and then gradually decrease with the increase of immersion time in all of the solutions at 80 °C.
- (4) The E_{corr} and E_{pit} tend to noble with the decrease of the concentration of chloride ion at the same temperature. The E_{pit} at 25 °C is much noble than that at 80 °C in the same solution.
- (5) The radius and depths of the pits formed on the surface after polarization curve tests are increase with the increase of concentration of chloride ions.

ACKNOWLEDGEMENTS

This work thank to the electric water heater research platform of Media.

References

1. S. C. Shi, C. C. Su, *Materials*, 9 (2016) 612.

2. S. J. Song, S. Cho, W. C. Kim, J. G. Kim, *Eng. Failure Anal.*, 87 (2018) 69-79.
3. R. S. Barot, P. Patel, A. Patel, A. Patel, *Mater. Today: Proc.*, 28 (2020) 1795-1800.
4. M. Zhang, R. Xu, L. Liu, S. Xin, M. Li, *Anti-Corros. Methods Mater.*, 67 (2020) 407-414
5. C. Bitondo, A. Bossio, T. Monetta, M. Curioni, F. Bellucci, *Corros. Sci.*, 87 (2014) 6-10.
6. T. Bellezze, G. Roventi, A. Quaranta, R. Fratesi, *Mater. Corros.*, 59 (2008) 727-731.
7. B. Zhang, S. Hao, J. Wu, X. Li, C. Li, X. Di, Y. Huang, *Mater. Charact.*, 131 (2017) 168-174.
8. R. Jiang, Y. Wang, X. Wen, C. Chen, J. Zhao, *Appl. Surf. Sci.*, 412 (2017) 214-222.
9. S. Cho, J. H. An, S. H. Lee, J. G. Kim, *Int. J. Electrochem. Sci.*, 15 (2020) 4406-4420.
10. Y. S. Choi, J. J. Shim, J. G. Kim *J. Alloys Compd.*, 391 (2005) 162-169.
11. H. Bi, G. T. Burstein, B. B. Rodriguez, G. Kawaley, *Corros. Sci.*, 102 (2016) 510-516.
12. C. Bitondo, A. Bossio, T. Monetta, M. Curioni, F. Bellucci, *Corros. Sci.*, 87 (2014) 6-10.
13. G. S. Vasyliiev, *Corros. Sci.*, 98 (2015) 33-39.
14. A. Fattah-Alhosseini, F. Soltani, F. Shirsalimi, B. Ezadi, N. Attarzadeh, *Corros. Sci.*, 53 (2011) 3186-3192.
15. R. T. Loto, C. A. Loto, *Journal of Materials Research and Technology*, 7 (2018) 231-239.
16. H. Luo, H. Su, B. Li, G. Ying, *Appl. Surf. Sci.*, 439 (2018) 232-239.
17. S. He, D. Jiang, *Int. J. Electrochem. Sci.*, 13 (2018) 5832-5849.
18. X. Y. San, B. Zhang, B. Wu, X. X. Wei, E. E. Oguzie, X. L. Ma, *Corros. Sci.*, 130 (2018) 143-152.
19. M. Lagarde, A. Billard, J. Creus, X. Feaugas, J. L. Grosseau-Poussard, S. Touzain, C. Savall, *Surf. Coat. Technol.*, 352 (2018) 581-590.
20. D. Zuili, V. Maurice, P. Marcus, *J. Electrochem. Soc.*, 147 (2000) 1393-1400.
21. Q. Zhou, Y. Wang, H. Wu, Q. Zhong and J. Jiang, *Surf. Coat. Technol.*, 207 (2012) 503-507.
22. L. Guan, B. Zhang, X. P. Yong, J. Q. Wang, E. H. Han, W. Ke, *Corros. Sci.*, 93 (2015) 80-89.
23. Q. Zhou, S. Liu, L. Gan, X. Leng and W. Su, *Mater. Res. Express*, 5 (2018) 116534.
24. Q. Zhou, S. Sheikh, P. Ou, D. Chen, Q. Hu, and S. Guo, *Electrochem. Commun.*, 98 (2019) 63.
25. H. Gerengi, K. Darowicki, G. Bereket, P. Slepski, *Corros. Sci.*, 51 (2009) 2573-2579.
26. H. Luo, Z. Li, A. M. Mingers, D. Raabe, *Corros. Sci.*, 134 (2018) 131-139.
27. S. Xin, R. Xu, H. Yan, P. Shen, M. Li, *Int. J. Electrochem. Sci.*, 14 (2019) 11012-11018.